

FIRST SILICON MICROTURBINE WITH INTEGRATED PERMANENT MAGNETS SUPPORTED ON ENCAPSULATED MICROBALL BEARINGS

Mustafa I. Beyaz^{1*}, B. Hanrahan², R. Ghodssi^{1,2}

MEMS Sensors and Actuators Laboratory

¹Department of Electrical and Computer Engineering, ²Department of Materials Science and Engineering
Institute for Systems Research, University of Maryland, College Park, MD USA

*Presenting Author: beyaz@umd.edu

Abstract: The design, fabrication, and testing of the first microball bearing supported silicon microturbine with integrated permanent magnets is reported. The device is composed of two bonded silicon wafers with encapsulated microball bearings and discrete magnetic components, measuring 6mm in radius. Initial tests with pressurized nitrogen as a driving mechanism show a linear relationship between the rotational speed and gas flow rate. A maximum speed of 24krpm has been achieved with the current test setup, demonstrating the capability of this device for microscale power conversion. The microturbine presented in this work will lead to fully integrated, high-speed, and robust MEMS platforms for high-density power generation.

Keywords: microturbine, microball bearings, microgenerator

INTRODUCTION

The development of small-scale high energy density power sources has become increasingly essential as the size of portable microsystems relying on these sources continues to shrink. In addition to microbatteries, a significant effort has been focused on the realization of power generators based on rotating micromachinery. In these devices, electromagnetics has been preferred over other transduction principles for highest output power, like that in macroscale systems [1-7].

Several microgenerators have been demonstrated with off-the-shelf bearing components to support the rotating part (rotor) of the device, providing output power in the range of milliwatts to watts [1-5]. For a fully integrated, compact, and functional microsystem, it is necessary to incorporate the bearing mechanism into device design and fabrication. Yen *et al.* developed an air bearing supported microturbine with permanent magnets and reported stable operation up to 40krpm [6]. A similar device with magneto-pneumatic bearings was presented by Raisigel *et al.* with a maximum speed of 58krpm [7].

As output power is proportional to the rotational speed squared to the first order, it is extremely advantageous to incorporate a stable and robust bearing mechanism that enables high speeds for rotational components housing magnetic materials. Encapsulated ball bearing support mechanism has been previously developed by our group for an air driven micro-turbo-pump and rotational speeds up to 87krpm have been demonstrated [8]. The friction and wear performance of a similar device reported in [9] shows the long-term reliability and robustness of these bearings. The focus of this work is to utilize the high-speed characteristics and robustness of the encapsulated microball bearings and develop a microturbine with integrated permanent magnets for the realization of high-power micro-turbo-generators.

DESIGN AND FABRICATION

The device presented in this work is composed of two bonded silicon wafers with encapsulated microballs ($\varnothing=285\mu\text{m}$) in between, and measures 6mm in radius. While the top wafer is dry-etched with turbine blade structures for pneumatic actuation, the bottom wafer provides housing for magnetic materials. The fabrication of the device is summarized in figure 1. Initially, top and bottom wafers were etched to create ball raceways that are $95\mu\text{m}$ and $195\mu\text{m}$ in depth, respectively (figure 1a). More than 80% of the raceways were then filled with microballs and the two wafers were bonded using a $1\mu\text{m}$ thick eutectic AuSn metal (figure 1b) deposited with thermal evaporation. Several etch steps were performed on both sides of this bonded stack to define the turbine blades, magnetic housing, and to release the rotor from outer silicon frame (figure 1c). The release lines are designed with a $90\mu\text{m}$ offset to allow the microballs to ride on smooth silicon surfaces.

Separately, ten discrete pie-shaped 0.5mm-thick NdFeB magnets, measuring 2mm in inner and 5mm in outer radii, were assembled on a 0.2mm-thick permendur (FeCoV) disc with the same outer radius. The magnets were placed in an alternating polarity to create time varying magnetic field as the turbine spins. NdFeB magnets were chosen for their high remanent flux density (up to 1.4T). The inclusion of the FeCoV disc simplifies the integration of the magnets into the rotor and improves the magnetic flux density due to its high magnetic permeability and saturation flux density. Next, the FeCoV disc with permanent magnets was bonded to the rotor housing using epoxy as shown in figure 1d.

In parallel, a third silicon chip (plumbing chip) was dry etched from both sides to define through-holes and a $50\mu\text{m}$ -deep recess on the bottom side (figure 1e). While the through-holes direct the pressurized gas flow into and out of the device, the recess on the back

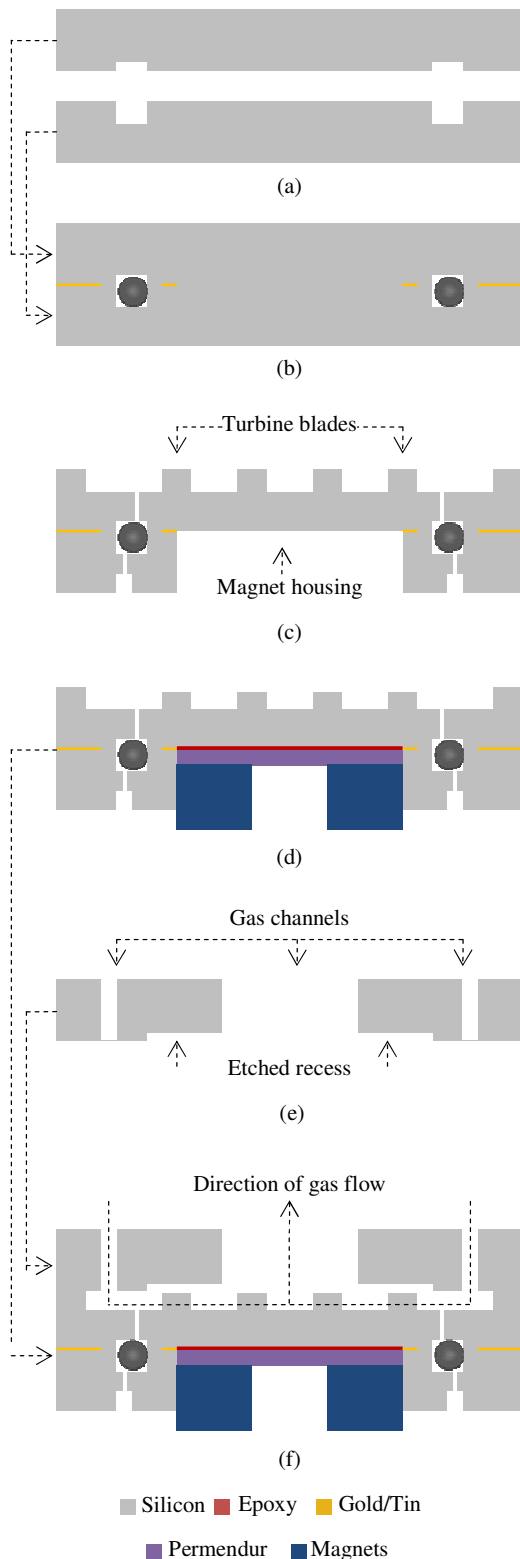


Figure 1. Fabrication flow that shows (a) etched ball housings on two wafers, (b) eutectic bonding of two wafers with microballs in the raceway, (c) etched turbine structures, magnet housing, and released rotor (d) NdFeB magnets and permendur (FeCoV) disc bonded in the rotor, (e) plumbing layer chip for directing gas flow, (f) complete device.

side prevents a possible collision between the turbine blades and the plumbing chip that may lead to catastrophic failure. Figure 1f is a schematic representation of the complete device showing individual components as well as the direction of gas flow.

Images of the top and bottom sides without the plumbing layer are shown in figures 2 and 3, respectively. In addition to the turbine structures, six radial features are defined on the top surface for speed measurements as shown in figure 2.

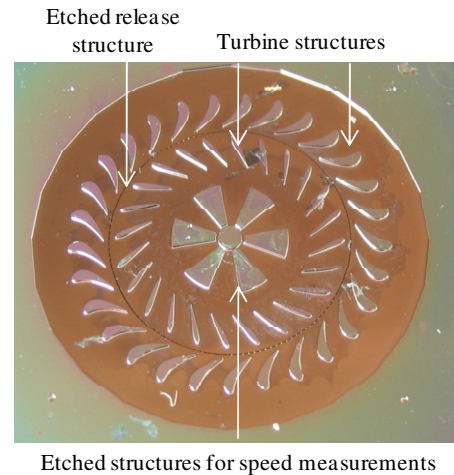


Figure 2. Photograph of the top side of the device showing the released rotor, turbine structures, and etched structures for speed measurements.

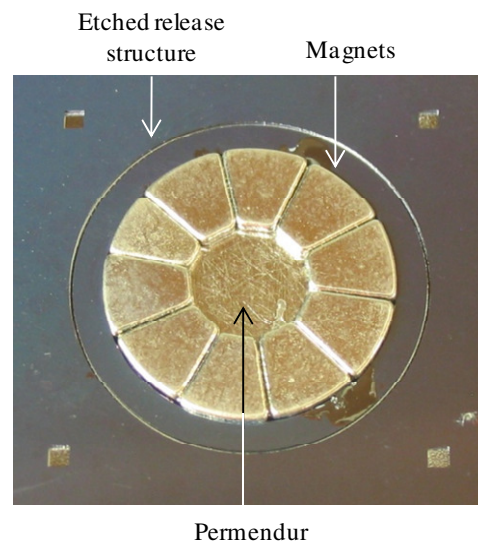


Figure 3. Photograph of the bottom side of the device showing the released rotor, permendur disc, and discrete pie shaped magnets.

RESULTS AND DISCUSSION

As pressurized gas is applied to the turbine during testing, the pressure distribution on the rotor results in a net force in the upward direction on figure 1f while the heavy magnetic materials are pulled by gravity. This would allow the total rotor weight to overcome

the air pressure at low speeds and lead the microballs to ride on sharp raceway corners that quickly wear away. Accordingly, the turbine is tested upside down for both forces to point the same direction that would result in the microballs to ride on the smooth silicon surface.

The picture of the packaged device is shown in figure 4. Lexan packaging is designed to facilitate pressurized nitrogen through fluidic ports, while simultaneously allowing for pressure, flow, and speed measurements. An optical probe is positioned on the bottom side, aligned vertically with the etched speed structures, to measure the reflectance change of these structures due to the spinning turbine. A LabVIEW virtual interface is designed to collect data from the optical probe as well as a mass flow meter, and to measure the rotational speed as a function of flow rate.

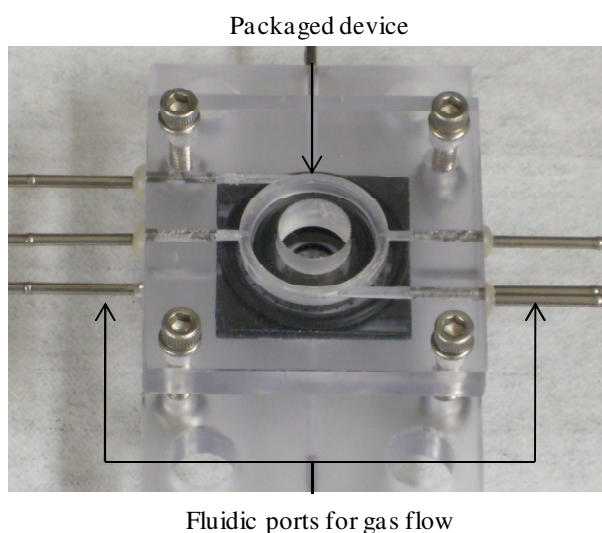


Figure 4. Picture of the packaged device with fluidic connections for pressurized gas flow.

Figure 5 shows the speed versus flow rate results of the initial tests performed on the device. The curve demonstrates an expected linear relationship with some erratic data which is attributed to the fabrication imperfections and residues that wear away during testing. A maximum speed of 24krpm has been achieved with the current test setup. This speed is lower than 87krpm previously demonstrated in [8] and can be improved through changes on the current test package and setup.

An important factor to notice is the higher flow rates required to spin this turbine in comparison to the similar devices reported in [8, 9] with 5mm radius. At 10krpm, the previously demonstrated devices required 0.4psi and 3slm while 0.4psi and 6slm was applied to the current device to reach the same speed. This is mainly due to the 44% increase in the area and silicon mass and longer race track housing more microballs as well as the magnetic materials that cause approximately four-fold increase in the total weight. This changes the dynamics of the device and as a

result, the torque, flow rate, and mechanical power required to drive the turbine increases.

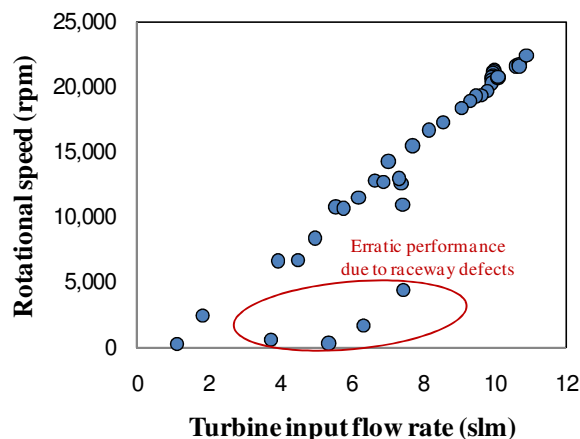


Figure 5. Microturbine performance graph that demonstrates a linear relationship between the flow rate and speed. Scattered data is a result of fabrication imperfections and residues that wear away during testing.

CONCLUSION

The device presented in this work is the first realization of a silicon microturbine with integrated microball bearings and magnetic materials. Microball bearings have been used for their high speed characteristics along with their robustness and stability, while NdFeB and FeCoV have been chosen for their high remanent flux density and saturation flux density/magnetic permeability, respectively. Initial tests on the 6mm-radius device showed a linear relationship between the flow rate and rotational speed, with a maximum value of 24krpm. This highest speed is currently limited by the test setup and can be improved through a number of modifications. Stability and robustness provided by ball bearings together with complete incorporation of magnets into the silicon rotor enables high-speed device operation and allows for the development of MEMS micro-turbo-generators with high-density power delivery capabilities.

ACKNOWLEDGEMENTS:

This work was supported by the National Science Foundation under Award No. 0901411. The authors would also like to acknowledge US Army Research Laboratory and Laboratory for Physical Sciences.

REFERENCES

- [1] Arnold D P, Herrault F, Zana I, Galle P, Park J W, Das S, Lang J H, Allen M G 2006 Design optimization of an 8 W, microscale, axial-flux, permanent magnet generator *J. Micromech. Microeng.* **16** S290-S296
- [2] Herrault F, Ji C H, Kim S H, Wu X, Allen G 2008 A microfluidic-electric package for Power MEMS generators *Technical Digest MEMS 2008*

- (Tucson, USA, 13-17 January 2008) 112-115.
- [3] Herrault F, Ji C H, Allen M G 2008 Ultraminiaturized, high-speed, permanent magnet generators for milliwatt-level power generation *J. Microelectromech. Syst.* **17** no 6, pp1376-1387.
- [4] Holmes A S, Hong G, Pullen K R 2005 Axial-flux permanent magnet machines for micropower generation *J. Microelectromech. Syst.* **14** no 1, pp54-62.
- [5] Pan C T, Wu T T 2007 Development of a rotary electromagnetic microgenerator *J. Micromech. Microeng.* **17** S120-S128.
- [6] Yen B C, Herrault F, Hillman K J, Allen M G, Ehrich F F, Jacobson S, Ji C H, Lang J H, Li H, Spakovszky S, Veazie D R, 2008 Characterization of a fully-integrated permanent-magnet turbine generator *Technical Digest PowerMEMS 2008 (Sendai, Japan, 9-12 November 2008)* 121-124.
- [7] Raisigel H, Cugat O, Delamare J 2006 Permanent magnet planar microgenerators *Sensors and Actuators A: Physical* **130** pp438-444.
- [8] Waits C M, McCarthy M, Ghodssi R 2010 A microfabricated spiral-groove turbopump supported on microball bearings *J. Microelectromech. Syst.* **19** no 1, pp99-109.
- [9] McCarthy M, Waits C M, Ghodssi R 2009 Dynamic friction and wear in a planar-contact encapsulated microball bearing using an integrated microturbine *J. Microelectromech. Syst.* **18** no 2, pp263-273.